Non-local MRI Library-Based Super-Resolution: Application to Hippocampus Subfield Segmentation

Jose V Romero, Pierrick Coupé, Jose V Manjón

Non-local MRI Library-based Super-resolution: Application to Hippocampus Subfield Segmentation

Jose E. Romero[1], Pierrick Coupé[2,3], Jose V. Manjón[1]

[1]Instituto de Aplicaciones de las Tecnologías de la Información y de las Comunicaciones Avanzadas (ITACA), Universitat Politècnica de València, Camino de Vera s/n, 46022, Valencia, Spain
[2] Univ. Bordeaux, LaBRI, UMR 5800, PICTURA, F-33400 Talence, France.
[3] CNRS, LaBRI, UMR 5800, PICTURA, F-33400 Talence, France.

Abstract. Magnetic Resonance Imaging (MRI) has become one of the most used techniques in research and clinical settings. One of the limiting factors of the MRI is the relatively low resolution for some applications. Although new high resolution MR sequences have been proposed recently, usually these acquisitions require long scanning times which is not always possible neither desirable. Recently, superresolution techniques have been proposed to alleviate this problem by inferring the underlying high resolution images from low resolution acquisitions. We present a new superresolution technique that takes benefit from the self-similarity properties of the images and the use of a high resolution image library. The proposed method is compared with related state-of-the-art methods showing a significant reconstruction improvement. Finally, we show the advantage of the proposed framework compared to classic interpolation when used for segmentation of hippocampus subfields.

1   Introduction

Magnetic resonance imaging (MRI) is a valuable tool in the study of many brain dysfunctions for different areas such as neurology and psychiatry. For instance, MRI enables to investigate specific structures such as the hippocampus. This structure is known to be an important biomarker for several pathologies like Alzheimer's disease [1]. However, the study of specific areas such as the hippocampus requires high-resolution images difficult to obtain in clinical practice. Interpolation based methods [2] have been used in the past to increase the apparent resolution. However, these techniques do not provide new information but just produce blurred versions of the corresponding high resolution images. The application of super-resolution techniques has demonstrated to improve image quality in MRI [3]. Nevertheless, these methods are usually based on multiple low-resolution acquisitions with small shifts that results in additional time and thus can be a limiting factor in clinical environments. Recently, single MRI superresolution techniques have emerged as an efficient and accurate way to improve image resolution [4,5]. These methods are often based on a nonlocal means framework [6] taking advantage of the intra-image pattern redundancy.

Manjón et al. presented a method called Non-local Upsampling [4] that improved effectively the image resolution by using a constrained reconstruction process based on image regularity and inter-scale coherence constraints to produced physically plausible results. Coupe et al. [7] further extended this method by using a local adaptive regularization that made the process more efficient and accurate.

In this work we propose an extension of Local Adaptive SR (LASR) method [7] that uses an external HR image library to take advantage from the intra and inter-image pattern redundancy at the same time. The method is compared to related state-of- the-art methods and the impact of SR on hippocampus subfield segmentation is also evaluated.

2   Material and Methods

As described in [4], MRI low resolution (LR) image voxels y can be related to the corresponding underlying high resolution (HR) voxels x through a simple degradation model:

$$y = DHx + n \tag{1}$$

where D is a decimation operator (defined as taking each Lth value starting from zero in each dimension), H is the convolution matrix (modeled as a 3D boxcar function), x is the underlying HR data, and n is random noise [4]. Therefore, the aim of any superresolution method is to infer the HR x_i values within each y LR voxel using some internal or external image information together with some reconstruction constraints.

2.1   Non-local Upsampling

In [4], the authors presented the Non-local Upsampling method. This SR method is able to infer a HR image by taking benefit of the self-similarity properties on the MR images. The SR method proposed in this paper is an improvement of this method that improves the HR image reconstruction by using a library of HR images. Briefly, Non-local Upsampling method infers the HR image iteratively by alternating two steps: 1) regularization and 2) mean correction.

First, the regularization consist of the application of a 3D non-local means filter which enforces the regularity of the image by estimating the value of each voxel as a weighted average of nearby voxels by using their patch similarity (see eq. 2 and 3).

$$x_p^{t+1} = \frac{1}{C_p} \sum_{q \in \Omega} w(x_p^t, x_q^t) x_q^t \tag{2}$$

$$w(x_p^t, x_q^t) = \begin{cases} e^{-\frac{\left\| N(x_p^t) - N(x_q^t) \right\|^2}{h^2}} & , if \left| \mu_p^t - \mu_q^t \right| < 3h / \sqrt{N} \\ 0, & otherwise \end{cases} \tag{3}$$

Where x_p^t is the voxel located at the position p of the actual image at iteration t, w measures the similarity between $N(x_p^t)$ and $N(x_q^t)$, the patches around voxels p and q, Ω is a restricted search volume surrounding the voxel being processed, Cp is a normalization constant, h is a filtering parameter related to the degree of smoothing and N is the number of voxels in each patch. Eq. (3) shows how the similarity between patches is estimated by preselecting patches with similar mean values μ_p^t.

Second, after the regularization step a mean correction step is necessary to enforce the inter-scale coherence (i.e. downsampled version of the inferred HR image has to be equal than the original LR image). To do so, Eq. (4) is applied.

$$\hat{x} = \hat{x} - NN(S(\hat{x}) - y) \tag{4}$$

where S is a downsampling operator that transforms actual reconstructed HR data to the original LR scale and NN is a nearest neighbor interpolation operation that interpolates LR data to HR scale. Due to the presence of noise, the constraint expressed in (4) cannot be directly used. To simplify the problem, LR data is first denoised using a non-local means filter [8] so the inter-scale constrain can be roughly met. For more details on the Non-Local Upsampling method, we refer the reader to the original paper [4]. This process (regularization-correction) is repeated iteratively using decreasing values of the filter parameter h until no significant differences are found.

2.2   Library-based Non-local Upsampling

One of the main limitations of the Non-Local Upsampling method is the fact that only the information contained within the image itself is taken into account while inter-image pattern redundancy could be useful as shown in [5].

In this paper, we extend the Non-Local Upsampling method by using a library of HR images that have the resolution desired after upsampling. Therefore, the training images and the image under study have to be preprocessed in a similar way. The steps included in this preprocessing are the following: 1) *Denoising*: The Spatially Adaptive Non-local Means (see [8]) Filter was applied to reduce the noise in the images. This filter is chosen because it is able to automatically consider stationary and spatially varying noise levels. 2) *Inhomogeneity correction*: The N4 bias field correction [9] was applied to correct intensity inhomogeneities across the image. 3) *MNI space affine registration*: The images are linearly registered to the Montreal Neurological

Institute (MNI) space using the MNI152 template. This was done using the Advanced Normalization Tools (ANTs) [10]. 4) *Subvolume cropping*: A cropping step is applied as the region of interest is significantly smaller than the image volume to reduce the computational burden of the method limiting the process to the area of interest. This step can be omitted if we are interested in the whole volume. *5) Subvolume Non-linear registration*: To achieve a better local anatomy matching between the target image and the image library the cropped volume of both (target and templates) is non-linearly registered to the cropped MNI152 atlas. The non-linear registration was performed using ANTs tool [10] using cross correlation similarity measure. 6) *Intensity normalization*: It is necessary to normalize the images in order to obtain the same intensity values across all subjects so similar patterns can be found among them by using an intensity based similarity metric. To this purpose, a simple mean and variance matching method was used so all the cases have the same mean and variance. This normalization needs only to be approximated since we will compensate any local difference during the reconstruction process as we will show later. *7) BSpline interpolation*: This step is done to produce the initial estimation (only for the case to be up-sampled not for the library cases).

Library-based Upsampling

Once the library and the case to be upsampled are in the same geometric space and intensity range, we can apply the regularization-correction scheme but this time including the HR image library in the process (see equation 5).

$$x_p^{t+1} = \mu_p + \frac{1}{C_p}\left(\sum_{q\in\Omega}w(x_p^t,x_q^t)(x_q^t-\mu_q) + \sum_{i=1}^{K}\sum_{q\in\Omega}w_L(x_p^t,x_{q,i})(x_{q,i}-\mu_{q,i})\right) \tag{5}$$

$$w_L(x_p^t,x_{q,i}) = \begin{cases} e^{-\frac{\left\|(N(x_p^t)-\mu_p^t)-(N(x_{q,i})-\mu_{q,i})\right\|^2}{h^2}}, & if\ \left|\mu_p^t-\mu_{q,i}\right| < 3h/\sqrt{N} \\ 0, & otherwise \end{cases} \tag{6}$$

where K is the number of cases in the library, $x_{q,i}$ is the voxel q of the HR image I and μ_p, μ_q and $\mu_{q,i}$ are the mean value of a 3x3x3 voxel patch around voxels p, q and q,i. Note that x^0 is initialized by BSpline interpolation.

The main difference between equation 2 and 5 is the inclusion of a library of HR cases in the reconstruction process. While first term is aimed to regularize the image the second tries to bring new texture from proper examples in the library. To compensate for the different mean values of the patches from the library the mean of every patch is subtracted so only high frequency information is transferred from the HR images to the reconstructed image.

2.3 Multiatlas non-local label fusion segmentation

In order to measure the impact of the SR preprocessing on further image analysis, we decided to evaluate the ability of the SR to produce better segmentations. Specifically, we applied a recent non-local multi-atlas label fusion segmentation method that uses an adaptation of PatchMatch method called OPAL [11]. OPAL has an efficient strategy to find patch correspondences between two or more images, combines multiple matches and performs late label fusion with different scales and features.

3 Experiments and results

For our experiments we used a public dataset consisting in 5 HR cases with their corresponding manual hippocampus subfield segmentations* [12]. Each case consists of T1- and T2-weighted images at 0.3 mm resolution.

These images were preprocessed as described in the previous section. Specifically, the native 0.3 mm images were registered to MNI space at 0.5 mm resolution, cropped, non-linearly registered and intensity normalized. To increase the size of the library left hippocampus cropped images were mirrored so the final library consists of 10 right hippocampus area images (10 for T1 and 10 for T2). We run two types of experiments:

1. *Reconstruction quality assessment*: In this experiment, the HR images were downsampled to have 1 mm resolution and later upsampled with the different methods to assess their quality.
2. *Segmentation accuracy assessment*: In this experiment, the different upsampling methods were evaluated in order to find out which was their impact on segmentation accuracy.

3.1 Superresolution reconstruction image quality assessment

For the first experiment, both T1 and T2 HR image libraries were used. A leave-two-out was used by removing from the library both hippocampi (left and right) belonging to the case being evaluated. We upsampled the 1 mm LR images to 0.5 mm resolution using 3 different methods, classic BSpline interpolation, LASR [7] and the proposed library-based SR method. Peak Signal to Noise Ratio (PSNR) was used to evaluate the results (tables 1and 2).

---

* Images obtained from http://cobralab.ca/atlases/Hippocampus

Table 1. Upsampling PSNR results of the 10 T1 cases. Best results in bold.   .

Method	Cases										
	1	2	3	4	5	6	7	8	9	10	Avg.
BSpline	26.06	27.22	30.98	28.46	28.83	27.69	29.26	29.06	28.27	26.83	28.27
LASR	27.72	28.40	32.50	30.01	29.92	29.05	30.00	30.58	29.97	29.51	29.77
Proposed	**30.89**	**29.96**	**34.41**	**32.28**	**31.72**	**31.01**	**31.83**	**32.18**	**31.50**	**30.80**	**31.66**

Table 2. Upsampling PSNR results of the 10 T2 cases. Best results in bold.

Method	Cases										
	1	2	3	4	5	6	7	8	9	10	Avg.
BSpline	29.95	30.13	29.64	29.38	30.23	29.82	31.12	30.47	29.31	29.54	29.96
LASR	31.64	31.44	31.72	30.85	31.62	32.02	32.75	32.29	31.36	31.93	31.76
Proposed	**32.98**	**32.60**	**32.58**	**31.74**	**32.96**	**33.65**	**34.15**	**33.60**	**32.07**	**32.62**	**32.89**

As can be noticed the proposed method obtained the best results in all the cases for both T1 and T2 libraries. The improvement of the proposed method over LASR was found to be significant (p<0.001). In Figure 1, an example of the SR results with the different methods is shown. Regarding the processing times, BSpline interpolation took 1 second to process, LASR around 20 seconds and the proposed method 5 minutes.
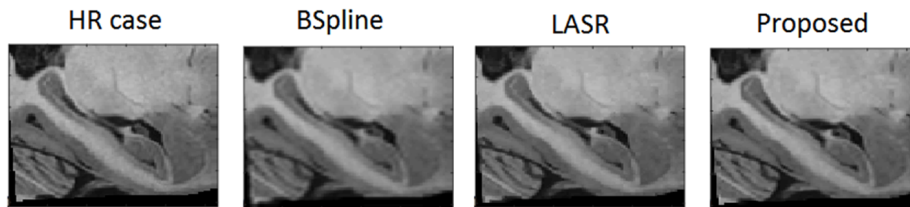
Fig. 1. Example of T1 SR results with the different methods. Note that both LASR and the proposed method produced a clearly better reconstruction than BSpline result (less blurry and more regular). Differences between LASR and the proposed method were not so obvious to assess visually (for example the white matter layer between hippocampus head and amygdala is better recovered by the proposed method).

3.2 Segmentation accuracy assessment

For the second experiment, we evaluated the accuracy improvement for a segmentation task obtained with the different upsampling methods. OPAL segmentation algorithm [11] was applied using default parameters to the original 10 HR T1 and T2 images (used as reference) and to the different upsampled results using BSpline, LASR and the proposed method over the images downsampled with a factor 2. Again, a leave-two-out was used by removing from the library both hippocampi (left and right) belonging to the case being evaluated. We used the DICE coefficient [13] to

measure the segmentation accuracy. In table 3 the segmentation results for the different subfields and for the whole hippocampus are shown.

Table 3. Segmentation results of the different methods compared (DICE). Best results in bold.

Method	Cases							
	T1 HR	T2 HR	T1 BSpline	T2 BSpline	T1 LASR	T2 LASR	T1 Proposed	T2 Proposed
CA1	0.6582	**0.7031**	0.6484	0.6826	0.6556	0.6935	0.6550	**0.6958**
CA2\CA3	**0.6725**	0.6261	0.6608	0.6061	0.6669	0.6176	**0.6681**	0.6195
CA4\DG	0.7035	**0.7538**	0.6932	0.7411	0.7020	0.7479	0.7019	**0.7499**
SR\SL\SM	0.4964	**0.5723**	0.4623	0.5401	0.4864	0.5539	0.4888	**0.5552**
Subiculum	0.5312	**0.6154**	0.5152	0.5830	0.5275	0.5980	0.5265	**0.6013**
Avg.	0.6124	**0.6541**	0.5960	0.6306	0.6077	0.6422	0.6081	**0.6443**
Whole	0.8752	**0.8843**	0.8701	0.8772	0.8742	**0.8817**	0.8738	0.8814

As expected, best results were found when using the T2 library. More importantly, we can clearly see how both SR methods improved significantly the segmentation results for both T1 and T2 cases compared to interpolation results. The proposed method improved subfield segmentation but not the whole hippocampus segmentation. Probably, SR helped to recover small details useful for subfield segmentation but not relevant to higher scale structures like the whole hippocampus.

4 Discussion

In this paper we presented a new super-resolution method that takes benefit from the use of an external HR image library to better reconstruct HR images from their corresponding LR counterparts. While LASR method was able to improve the image quality using the information within the image in form of a smart regularization, the proposed method is able to further improve these results by adding external information from similar examples in the library. More importantly, we have shown that both LASR and the proposed method are able to improve segmentation accuracy compared to simple BSpline interpolation and open the door to analyze retrospective LR data with a new insight. Although the improvement of the proposed method over LASR method is relatively small we have to note that we were using a small library (just 8 HR cases) and therefore we expect that using a larger library we will be able to represent more anatomical variability resulting in better results.

5   Acknowledgements

6   References

1. Braak H, Braak E, Neuropathological stageing of Alzheimer-related changes, Acta Neuropathol., 82 (4), pp. 239–259, (1991)
2. Thévenaz P, T. Blu, and M. Unser, "Interpolation revisited," IEEE Transactions on Medical Imaging, vol. 19, no. 7, pp. 739–758, (2000).
3. Carmi E, S. Liu, N. Alon, A. Fiat, and D. Fiat, "Resolution enhancement in MRI," Magnetic Resonance Imaging, vol. 24, no. 2, pp. 133–154, 2006.
4. Manjón, J. V, Coupé, P., Buades, A., Fonov, V., Collins, D.L., Robles, M.: Non-local MRI upsampling. Med. Image Anal. 14, 784–92 (2010a).
5. Manjón J.V., Coupé P, Buades A, Collins D.L., and Robles M, MRI Superresolution Using Self-Similarity and Image Priors, International Journal of Biomedical Imaging. Volume 2010 (2010b)
6. Buades A, Coll B, and Morel J.-M., "A non-local algorithm for image denoising," in Proceedings of the IEEE Computer Society Conference on Computer Vision and Pattern Recognition (CVPR '05), vol. 2, pp. 60–65, (2005).
7. Coupé P, Manjon J. V., Chamberland M, Descoteaux M. Collaborative patch-based super-resolution for diffusion-weighted images. NeuroImage,83:245-261, (2013).
8. Manjón J. V., Coupé P., Martí-Bonmatí L., Robles M, Collins L. Adaptive Non-Local Means Denoising of MR Images with Spatially Varying Noise Levels. Journal of Magnetic Resonance Imaging, 31,192-203, (2010)
9. Tustison, N.J., Avants, B.B., Cook, P.A., Zheng, Y., Egan, A., Yushkevich, P.A. and Gee, J.C. N4ITK: improved N3 bias correction. *IEEE Trans Med Imaging* 29(6): 1310 - 1320. (2010)
10. Avants, B.B., Tustison, N. and Song, G. Advanced normalization tools (ANTS). *Insight Journal.* (2009)
11. Giraud r, V-T. Ta, N. Papadakis, Manjón J. V., Collins D. L., Coupé P. and ADNI. An Optimized PatchMatch for Multi-scale and Multi-feature Label Fusion. NeuroImage, 124:770-782, (2016).
12. Winterburn l, Pruessner J.C., Chavez S, Schira M, Lobaugh N, Voineskos A, M. Chakravarty M, A novel in vivo atlas of human hippocampal subfields using high-resolution 3 T magnetic resonance imaging, NeuroImage, Vol74, 254-265, (2013)
13. Zijdenbos A.P., Dawant B. M., Margolin R. A., and Palmer A. C. Morphometric analysis of white matter lesions in MR images: method and validation. IEEE Transactions on Medical Imaging, 13(4): 716–724, (1994)